Supporting Information for:

Spectroscopic and Computational Studies on the Rearrangement of Ionized [1.1.1]Propellane and Some of its Valence Isomers: The Key Role of Vibronic Coupling

B. Müller,[†] T. Bally,*,[†] R. Pappas[§] and F. Williams*,[§]

Department of Chemistry, University of Fribourg, Switzerland and Department of Chemistry, University of Tennessee, Knoxville (USA).

CONTENTS

[†] University of Fribourg
[§] University of Tennessee

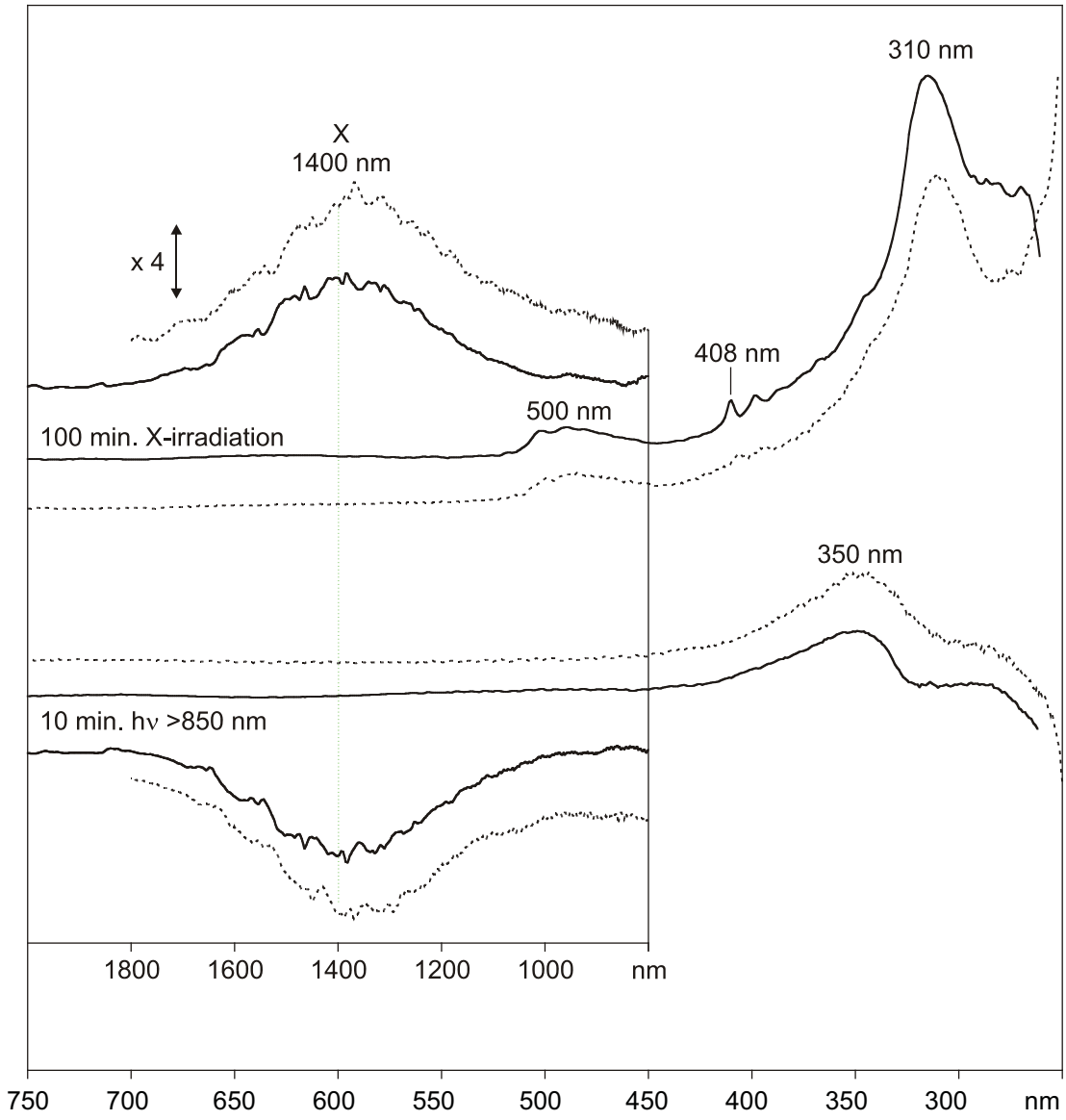

Figure S1: Comparison of the difference spectra obtained for the ionization and for the subsequent NIR bleaching of **1** (dotted line, corresponds to Figure 3 in the paper) and **2** (solid line) in Ar matrix. Apart from the group of peaks originating at 408 nm the two sets of spectra are largely identical.

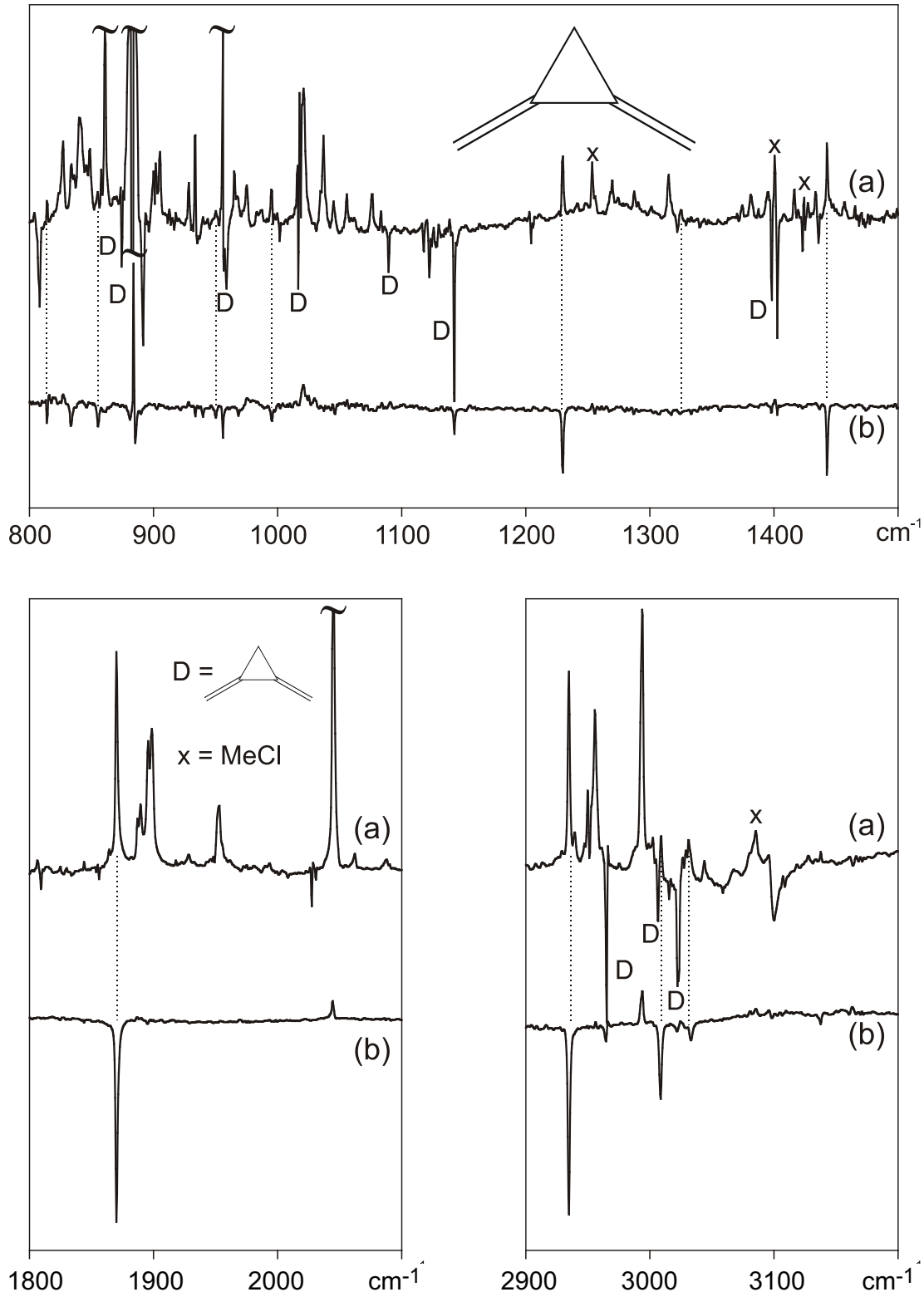

Figure S2: IR difference spectra for the radiolysis and subsequent NIR bleaching of **2** (cf. Figure 4 in the paper which shows the same for **1**).

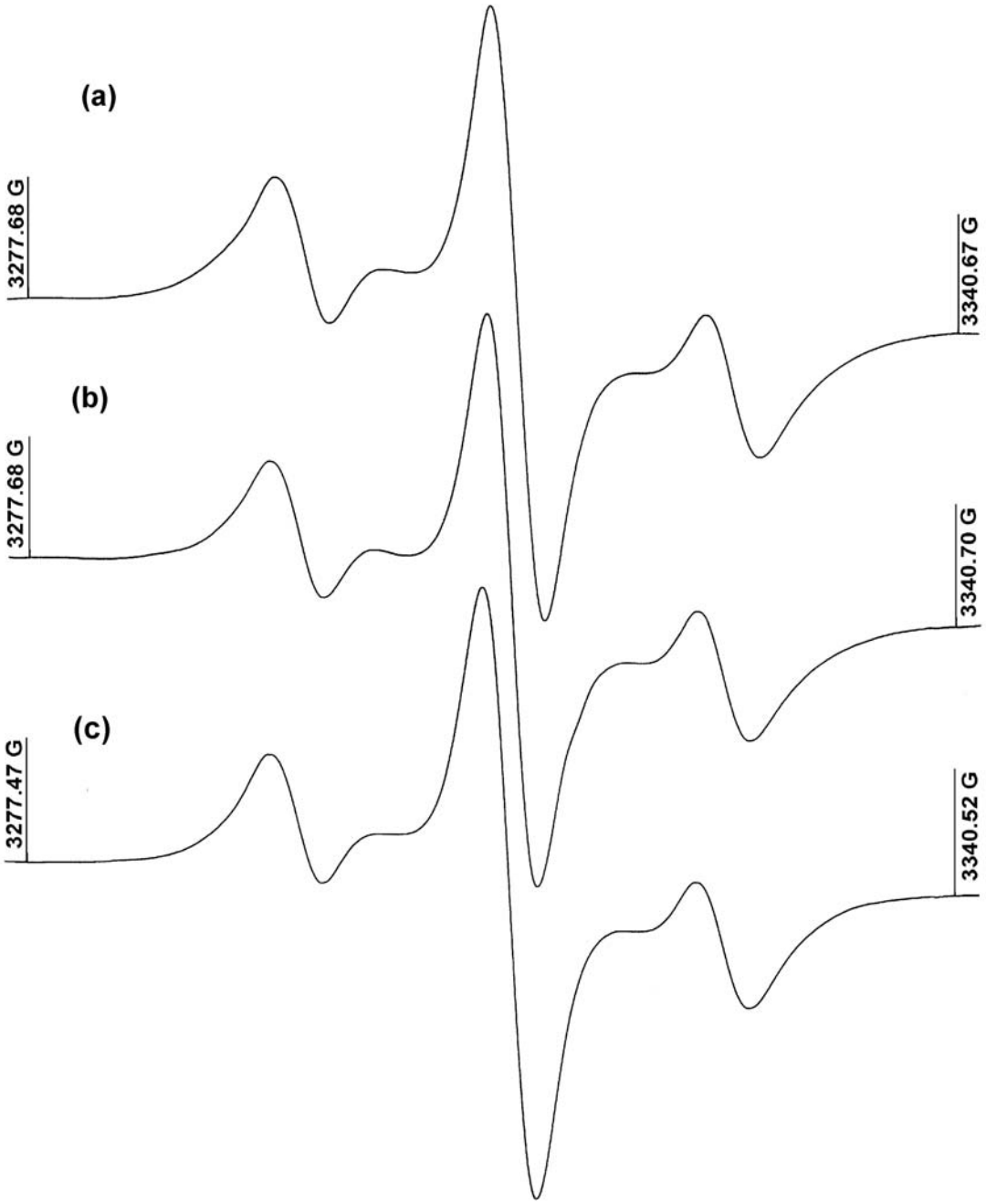

Figure S3: ESR spectra in CF2ClCCl3 at 100 K obtained after γ-irradiation and subsequent NIR photolysis of (a) propellane and (b) dimethylenecyclopropane. Both (a) and (b) are identical to, and exhibit the same alternating linewidth behavior as, the spectrum (c) obtained after gamma-irradiation of vinylidenecyclopropane.

Table S1: Experimental and computational values of the hyperfine coupling constants obtained for the radical cations **3**$^{\bullet+}$ and **4**$^{\bullet+}$, as well as for the corresponding neutral radical species **B** and **C** generated by the loss of a proton from the radical cation. The values for the latter are compared with those from the literature for prototype species.

Species	Hyperfine couplings / G	Reference
3$^{\bullet+}$	14.8 ($2H_{exo}$+$2H_{endo}$ not resolved), 5.4 (2H)	a
	-15.1 ($2H_{exo}$), *-15.8* ($2H_{endo}$), *-6.4* (2H)	*a*
B	14.6 ($2H_{exo}$ + $2H_{endo}$ not resolved)	a
CH_2=CH-CH_2•	14.8 ($2H_{exo}$), 13.9($2H_{endo}$)	b
CH_2=C(CH_3)-CH_2•	14.7 ($2H_{exo}$), 13.8($2H_{endo}$)	b
4$^{\bullet+}$	14.6 (2H from coupling to 2 diagonally placed cyclopropyl H-atoms in a twisted allene structure at 100 K)) 7.3 (4H from coupling to 4 cyclopropyl H-atoms, resulting from rapid equilibration of the two twisted enantiomers at 130 K) *18.2* (2H) *-2.8* (2H)	a a *a*
C	21.2 (4H) 12.2 (1H)	a
	22.0 (4H) *-15.7* (1H)	*a*
Me(H)C=C=CH•	19.6 ($3H_{Me}$), 18.7($1H_{alkene}$), 11.8 ($1H_{alkyne}$)	c

[a] This work (experimental); [*a*] This work (calculated by B3LYP/6-31G*); [b] Krusic, P. J.; Kochi; J. K. *J. Am. Chem. Soc.* **1968**, *90*, 7157; [c] Kochi; J. K.; Krusic, P. J. *J. Am. Chem. Soc.* **1970**, *92*, 4110.

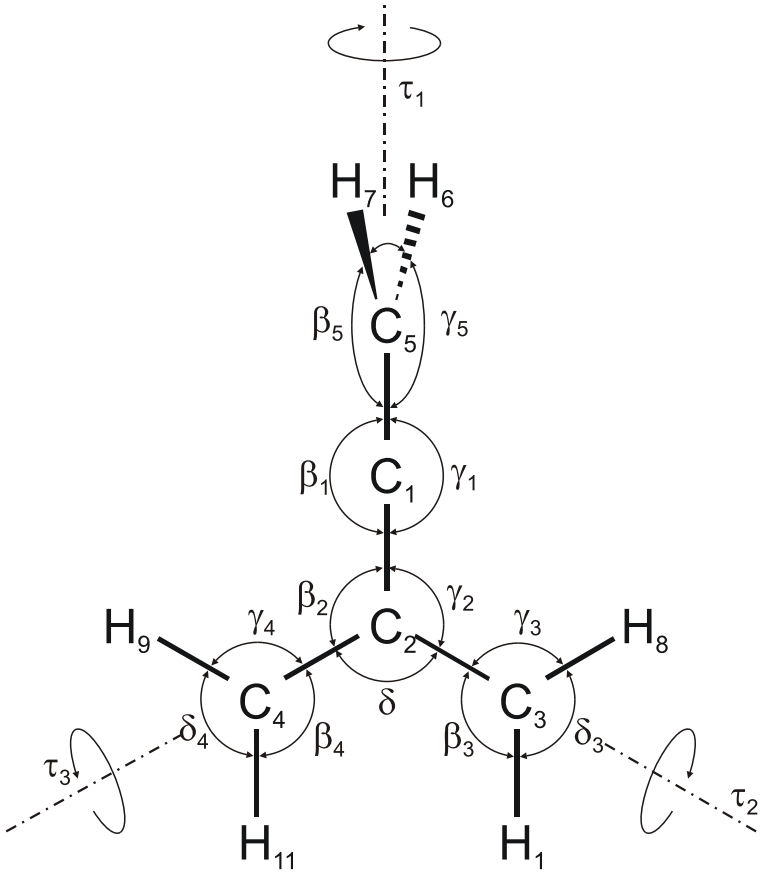

Figure S4: Internal valence coordinates of $\mathbf{3}^{\bullet+}$ which are used to define the symmetry-adapted internal coordinates in Table **S1** below.

Table S2: Definition of symmetry-adapted internal coordinates of $\mathbf{3}^{\bullet+}$ for use in the SQM procedure.

internal coord.[a]	description	composition	symmetry coord. a_1	a_2	b_1	b_2	scaling factors
R_1	ν(C-C)	$r(C_1\text{-}C_2)$	S_1				
R_2	"	$r(C_2\text{-}C_3)$	S_2			S_{20}	0.9303
R_3	"	$r(C_2\text{-}C_4)$					
R_4	ν(C=C)	$r(C_1\text{-}C_5)$	S_3				
R_5	ν(C-H)	$r(C_5\text{-}H_6)$	S_4		S_{14}		
R_6	"	$r(C_5\text{-}H_7)$					
R_7	"	$r(C_3\text{-}H_8)$	S_5			S_{21}	0.8936
R_8	"	$r(C_4\text{-}H_9)$					
R_9	"	$r(C_3\text{-}H_{10})$	S_6			S_{22}	
R_{10}	"	$r(C_4\text{-}H_{11})$					
R_{11}	$\delta(C\text{-}C\text{-}C)_{ip}$	$\beta_1\text{-}\gamma_1$				S_{23}	
R_{12}	$\sigma(C(CH_2)_2)$	$2\delta_2\text{-}\beta_2\text{-}\gamma_2$	S_7				0.9500
R_{13}	$\rho(C(CH_2)_2)$	$\beta_2\text{-}\gamma_2$				S_{24}	
R_{14}	$\sigma(CH_2)$	$2\delta_3\text{-}\beta_3\text{-}\gamma_3$	S_8			S_{25}	0.9474
R_{15}	"	$2\delta_4\text{-}\beta_4\text{-}\gamma_4$					
R_{16}	"	$2\delta_5\text{-}\beta_5\text{-}\gamma_5$	S_9				0.8653
R_{17}	$\sigma(CH_2)$	$\beta_3\text{-}\gamma_3$	S_{10}			S_{26}	0.9474
R_{18}	"	$\beta_4\text{-}\gamma_4$					
R_{19}	"	$\beta_5\text{-}\gamma_5$			S_{15}		0.8653
R_{20}	$\omega(CH_2)$	$\varepsilon_{2\text{-}3,8,10}$		S_{11}	S_{16}		0.9474
R_{21}	"	$\varepsilon_{2\text{-}4,9,11}$					
R_{22}	"	$\varepsilon_{1\text{-}5,6,7}$				S_{27}	0.8653
R_{23}	$\omega(C(CH_2)_2)$	$\varepsilon_{1\text{-}2,3,4}$			S_{17}		
R_{24}	$\delta(C\text{-}C\text{-}C)_{oop}$	$\beta_1'\text{-}\gamma_1'$ [b]			S_{18}		
R_{25}	τ(C=C)	$\tau_1(C_5H_{6,7})$		S_{12}			0.9500
R_{26}	τ(C-C)	$\tau_2(C_3H_{8,10})$		S_{13}	S_{19}		
R_{27}	"	$\tau_3(C_4H_{9,11})$					

[a] see Figure S4 abvoe, except for the wagging coordinates $\varepsilon_{i\text{-}j,k,l}$ which are devined as atom *i* moving perpendicular to the plane defined by atoms *j*, *k*, and *l*.
[b] $\beta_1'\text{–}\gamma_1'$ is perpendicular to $\beta_1\text{–}\gamma_1$

Table S3: Frequencies from SQM force field of $\mathbf{3}^{\bullet+}$ with scaling factors S_1-S_{27} optimized by fitting all observed peaks of $\mathbf{3}^{\bullet+}$

nr.	sym.	SQM [cm^{-1}]	obs. [cm^{-1}]	Δ[a] [cm^{-1}]	int.[b] [%]	int. [km/mol]	potential energy distribution[c]
1	a_1	3125.0			2.6	7.7	6(58)+5(42)
2	a_1	3021.9			0.1	0.4	5(58)+6(42)
3	a_1	2948.1	2935.0	13.1	66.2	192.3	4(99)
4	a_1	1870.5	1870.4	0.1	100.0	290.4	3(70)+1(28)
5	a_1	1468.2			1.0	2.9	8(92)+2(7)
6	a_1	1320.1			9.9	28.8	1(24)+10(21)+2(20)+9(12)+ 7(11)+3(10)
7	a_1	1227.9	1229.7	-1.8	26.5	76.9	9(87)+10(6)
8	a_1	994.0	995.7	-1.7	14.9	43.1	10(52)+2(40)+1(6)
9	a_1	795.6			0.3	0.8	1(41)+2(34)+3(14)+10(8)
10	a_1	376.9			0.7	2.0	7(82)+10(15)
11	a_2	836.8			0.0	0.0	11(99)
12	a_2	490.2			0.0	0.0	13(52)+12(38)+11(10)
13	a_2	254.4			0.0	0.0	12(52)+13(47)
14	b_1	3015.1	3033.6	-18.5	26.0	75.6	14(99)
15	b_1	863.2			3.7	10.8	16(51)+15(23)+18(13)+17(12)
16	b_1	853.6	856.5	-2.9	23.5	68.3	16(54)+15(33)+18(10)
17	b_1	523.2			2.5	7.2	19(42)+17(40)+18(8)+15(6)
18	b_1	459.1			0.0	0.1	19(35)+15(34)+18(16)+17(14)
19	b_1	223.8			2.7	7.9	18(43)+17(30)+19(19)+15(7)
20	b_2	3124.3			0.5	1.5	22(58)+21(41)
21	b_2	3015.1	3009.3	5.8	23.4	68.0	21(58)+22(41)
22	b_2	1441.8	1442.5	-0.7	20.8	60.5	25(94)+20(6)
23	b_2	1324.8	1324.7	0.1	11.9	34.5	20(80)+23(9)+26(8)
24	b_2	954.0	950.3	3.7	6.5	18.8	26(89)+20(11)
25	b_2	817.7	814.6	3.1	23.9	69.9	27(98)
26	b_2	506.2			6.9	20.1	23(48)+24(39)+20(7)
27	b_2	174.0			2.9	8.5	24(58)+23(40)

[a] RMS deviation of observed from calculated frequencies is 7.08 cm^{-1}.
[b] Intensities in % of the most intense band at 1870 cm^{-1}.
[c] Contributions in percent (in parentheses) of the symmetry coordinates listed in Table S1 above

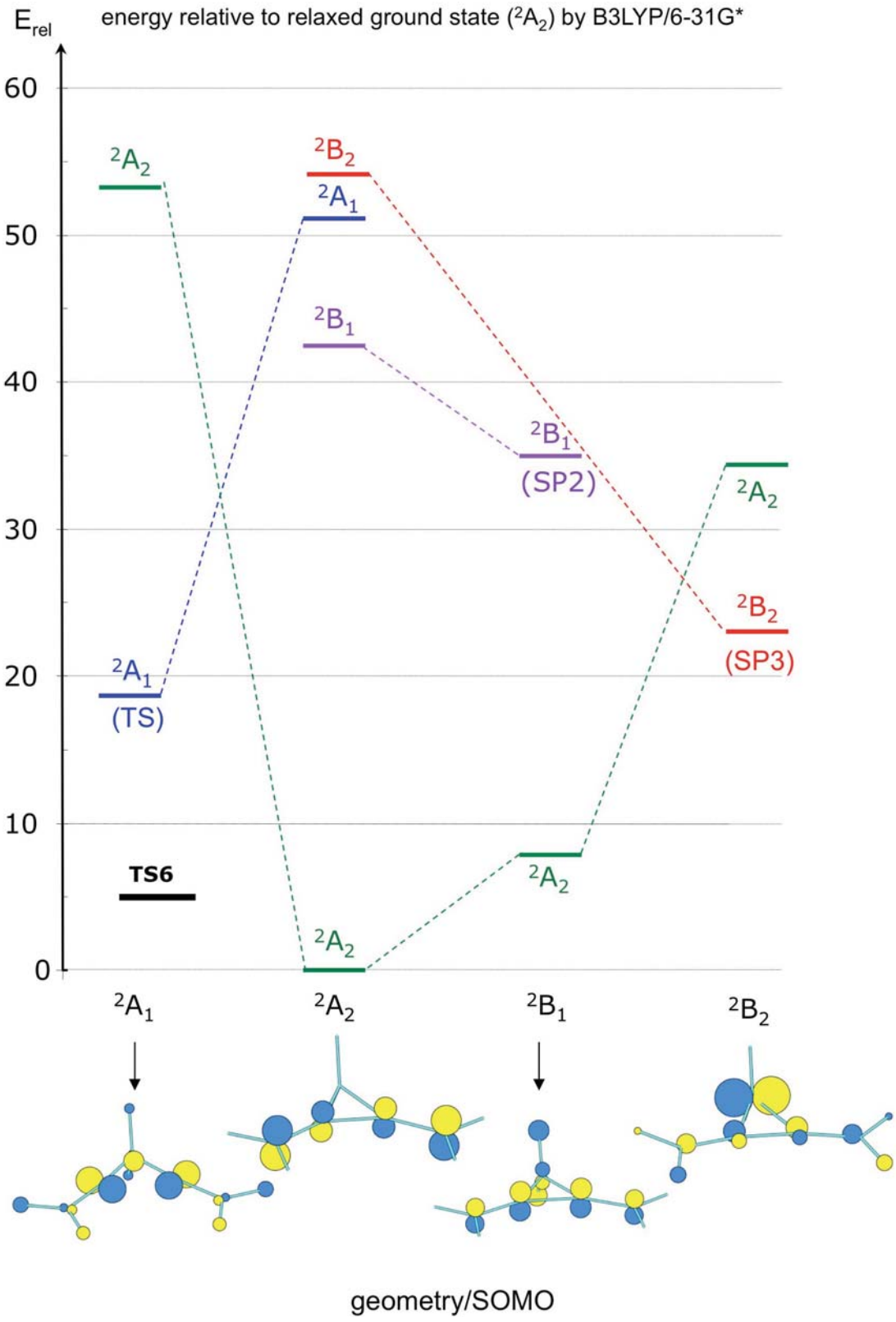

Figure S5: Relative energies of different excited states at the optimized geometries of the four lowest states of each symmetry of $\mathbf{2}^{\bullet+}$ ($^2A_2$ is the ground state). Note that no state crossing occurs anywhere near the energy where the transition state **TS6** for the rearrangement of $\mathbf{2}^{\bullet+}$ to $\mathbf{3}^{\bullet+}$ lies.

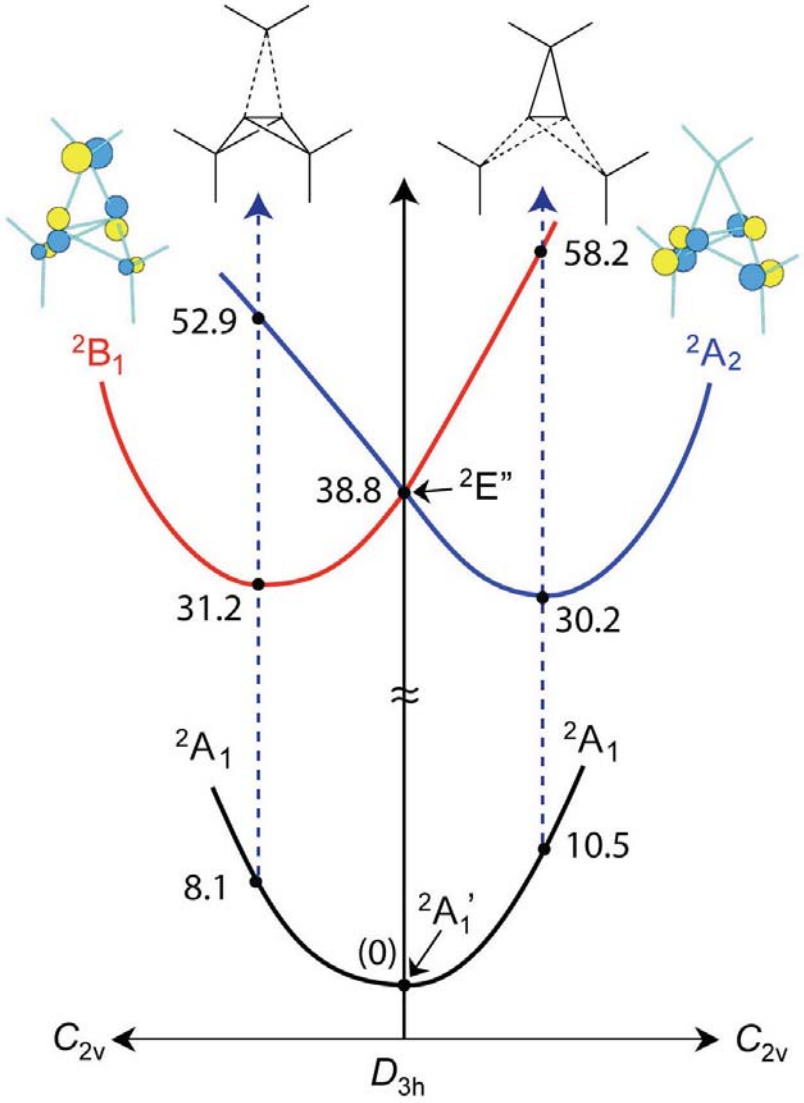

Figure S6: Potential surfaces for Jahn-Teller distortion of the $^2E''$ excited state of $\mathbf{1}^{\bullet+}$ along two components of an e' mode according to B3LYP/6-31G* calculations. The 2B1 stationary point is a transition state, the $^2A_2$ stationary point is a second-order saddle point. The two MOs are the respective SOMOs in the two states.

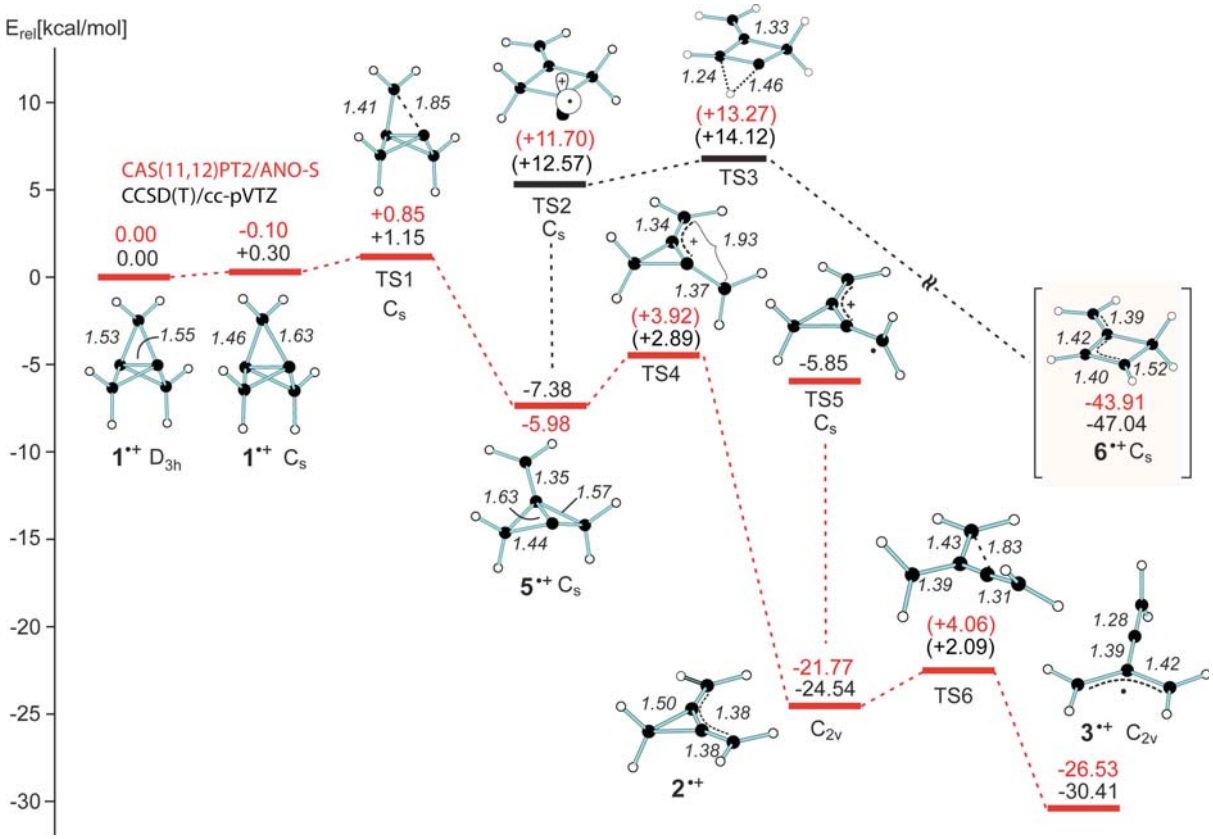

Figure S7: Figure 10 with relative CASPT2 energies (see Table S4) added in red. In all cases the ground state was described to ca 90% by a single configuration in the CAS(11,12) calculations, and no excited configuration contributed more than 4%. The CASPT2 wavefunction was described in all cases to 85-87%

Table S4: Results of CAS(11,12)SCF and CASPT2 calculations:

	CASSCF energy	CASPT2 energy	ref. weight[a]	G.S. weight[b]	large xs contrib.[c]	ΔE/kcal[d] (ex. ZPE)	B3LYP ZPE[e]	ΔE/kcal[d] (inc. ZPE)
1$^{\bullet+}$ D_{3h}	-192.53291	-192.99528	0.855	0.904	0.016	0.00	0.09097	0.00
1$^{\bullet+}$ C_s	-192.54514	-192.99613	0.861	0.896	0.013	-0.53	0.09165	-0.10
TS1	-192.54671	-192.99449	0.862	0.888	0.008	0.50	0.09154	0.85
5$^{\bullet+}$	-192.55440	-193.00311	0.859	0.887	0.032	-4.91	0.08927	-5.98
TS2	-192.51412	-192.98101	0.854	0.909	0.038	8.96	0.08581	5.72
TS3	-192.52437	-192.97885	0.857	0.891	0.033	10.31	0.08615	7.29
TS4	-192.55279	-192.99500	0.860	0.880	0.014	0.18	0.08740	-2.06
2$^{\bullet+}$	-192.55946	-193.02686	0.853	0.880	0.028	-19.81	0.08786	-21.77
TS6	-192.58453	-193.01928	0.861	0.873	0.014	-15.06	0.08674	-17.71
3$^{\bullet+}$	-192.60163	-193.03270	0.862	0.849	0.038	-23.48	0.08611	-26.53
6$^{\bullet+}$	-192.60558	-193.06506	0.857	0.903	0.017	-43.79	0.09077	-43.91

[a] weight of zero-order CASSCF wavefunction in the CASPT2 wavefunction; [b] squared coefficient of the ground-state configuration in the CASSCF wavefunction; [c] squared coefficient of the excited state wavefunction that has the largest contribution to the ground state CASSCF wavefunction; [d] energy relative to **1**$^{\bullet+}$ in D_{3h} symmetry; [e] zero-point energy from B3LYP/6-31G* calculation.